Electrochemistry Communications 108 (2019) 106565

Contents lists available at ScienceDirect

Electrochemistry Communications

journal homepage: www.elsevier.com/locate/elecom

Strengthening dendrite suppression in lithium metal anode by in-situ construction of Li–Zn alloy layer

Yingxin Lin[a], Zhipeng Wen[b], Chaochao Yang[a], Peng Zhang[a,*], Jinbao Zhao[a,b,*]

[a] College of Energy & School of Energy Research, Xiamen University, Xiamen 361102, China
[b] State Key Lab of Physical Chemistry of Solid Surfaces, Collaborative Innovation Centre of Chemistry for Energy Materials, State-Province Joint Engineering Laboratory of Power Source Technology for New Energy Vehicle, Engineering Research Center of Electrochemical Technology, Ministry of Education, College of Chemistry and Chemical Engineering, Xiamen University, Xiamen 361005, China

ARTICLE INFO

Keywords:
Li metal
Li–Zn alloy layer
Interface
Dendrite
Charge transfer kinetics

ABSTRACT

The lithium metal anode is one of the most attractive candidates for high-energy lithium rechargeable batteries because it has an ultrahigh theoretical specific capacity and the lowest electrode potential. Unfortunately, uncontrollable growth of dendritic Li leads to problems such as safety hazards and low cycling reversibility, which greatly hinder its commercial application. Here, a Li–Zn alloy layer is constructed in situ on Li metal foil by a simple chemical reaction of zinc trifluoromethanesulfonate with Li metal. The modified Li metal anode forms an interface with fast charge transfer kinetics and high chemical resistance to the electrolyte, which enables deposition of Li with a smooth, dense morphology without the growth of dendritic Li. In symmetrical cells, the Li metal anode with the Li–Zn alloy layer can reach a cycling lifetime of more than 500 h under a current density of 2 mA cm^{-2}. This work provides a simple and effective strategy to suppress the formation of Li dendrites.

1. Introduction

Lithium-ion secondary batteries have been widely used in electronic consumer products and electric vehicles [1]. However, with the development of long-range electric vehicles and large-scale energy storage systems, existing lithium-ion secondary batteries using graphite as an anode material cannot provide the required energy density [2,3]. The Li metal anode has become one of the most attractive candidates for high-energy rechargeable batteries because it has an ultrahigh theoretical specific capacity (3860 mAh g^{-1}) and the lowest electrode potential (−3.04 V vs. standard hydrogen electrode) [4].

Unfortunately, commercial application of Li metal anodes is fundamentally limited by safety hazards and low cycling reversibility caused by uncontrollable growth of Li dendrites [5]. Li metal anodes, which are “hostless” electrodes, in contrast to graphite anodes, undergo a virtually infinite relative volume change during repeated plating and stripping, and thus a stable interface between the highly reductive Li anode and the electrolyte cannot form [6]. In addition, this nonuniform and fragile solid electrolyte interphase (SEI) causes inhomogeneous Li ion flux, accelerating uneven deposition of Li ions and finally resulting in growth of dendritic Li [7]. Once dendritic Li penetrates the separator, serious safety problems such as thermal runaway and cell combustion can occur [4]. In addition, adverse reactions between dendritic Li and the electrolyte also exacerbate the formation of “dead” Li, which increases Li loss and results in a low coulombic efficiency [5]. Obviously, a good Li electrode/electrolyte interface with tailored electrochemical and mechanical properties, such as fast Li^+ diffusion and high interfacial stability, is essential for stabilizing the uniformity of Li metal during cycling.

In recent years, various methods have been proposed to improve the interfacial stability of Li metal anodes and inhibit growth of dendritic Li. Three-dimensional conductive network [8], electrolyte additives (vinylene carbonate [9] or 4-vinyl-1,3-dioxolan-2-one [10]), artificial coating layer (LiF [11], Li–Al [12], Li–Si [13], silane-based coatings [14]), are applied to improve the uniformity of Li deposition and suppress Li dendrite growth.

Here, we adopt a simple chemical method to construct a Li–Zn alloy layer in situ on the surface of the Li metal anode by applying zinc trifluoromethanesulfonate (ZnTFS) as a suitable source of zinc. More specifically, the resulting Li–Zn alloy layer facilitates fast charge transfer and reaction kinetics at the interface, which afford stable homogeneous deposition of Li and thus result in deposition of Li with a smooth morphology and no dendrite growth. In addition, the Li–Zn alloy is much more inert with respect to the electrolyte than Li alone, reducing side reactions between Li and the electrolyte. In symmetrical cells, the Li metal anode modified by a Li–Zn alloy layer can be cycled

* Corresponding authors.
E-mail addresses: pengzhang@xmu.edu.cn (P. Zhang), jbzhao@xmu.edu.cn (J. Zhao).

https://doi.org/10.1016/j.elecom.2019.106565
Received 29 August 2019; Received in revised form 23 September 2019; Accepted 11 October 2019
Available online 21 October 2019
1388-2481/ © 2019 The Author(s). Published by Elsevier B.V. This is an open access article under the CC BY-NC-ND license (http://creativecommons.org/licenses/BY-NC-ND/4.0/).

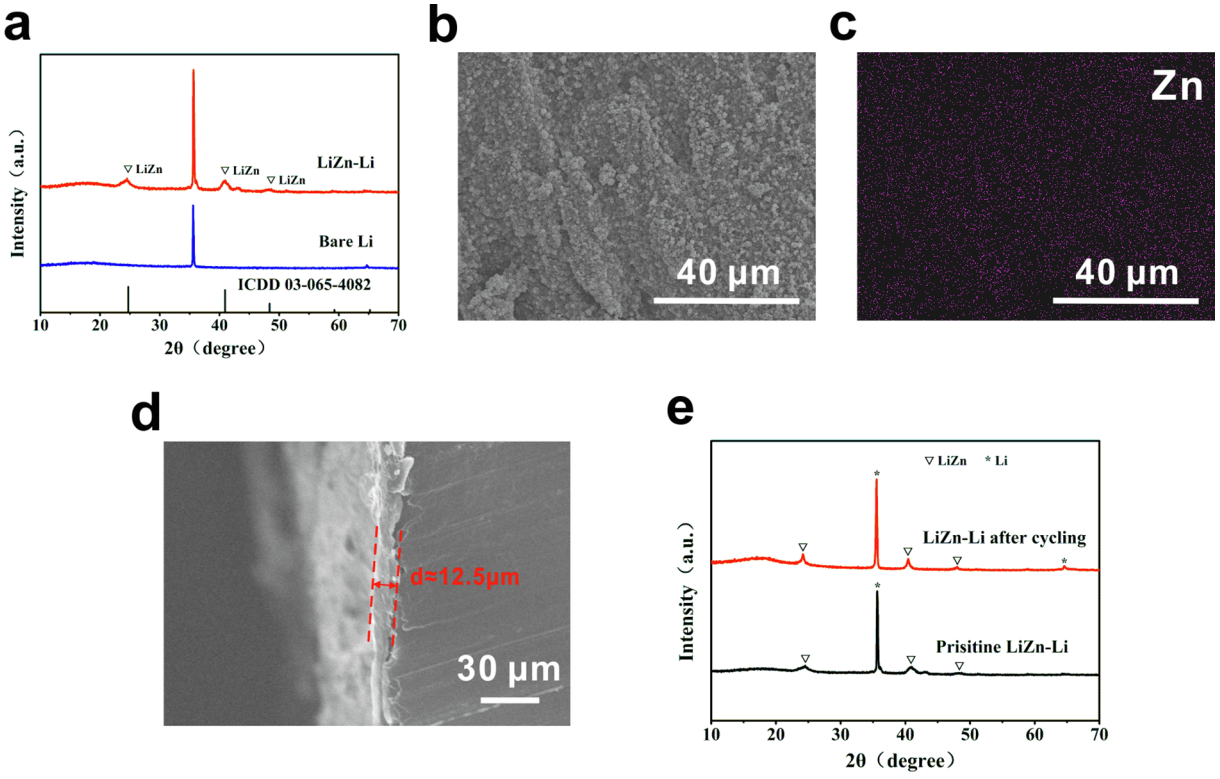

Fig. 1. (a) XRD patterns of LiZn-Li foil and bare Li foil. (b) SEM image of surface of LiZn-Li foil; (c) EDS elemental mapping of Zn on surface of LiZn-Li foil; (d) Cross-section SEM image of LiZn-Li foil. (e) XRD pattern of LiZn-Li electrode after cycling.

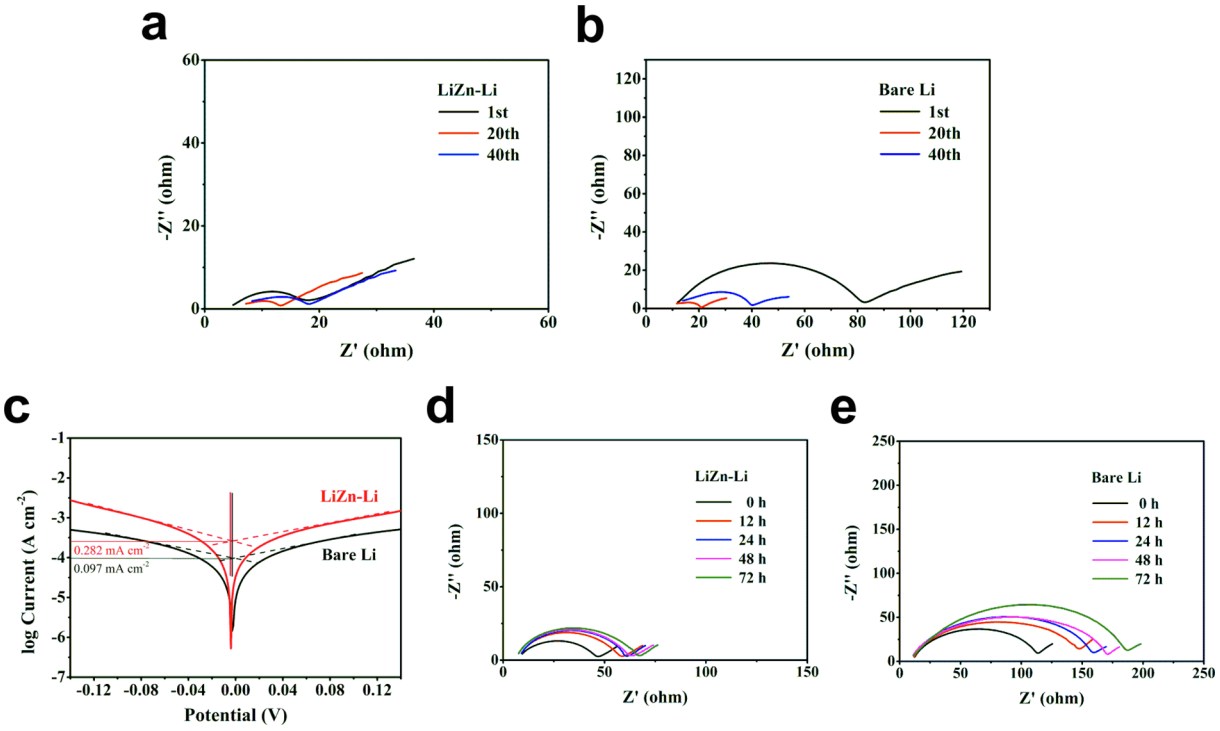

Fig. 2. EIS spectra of symmetric cells at different cycles for (a) LiZn-Li electrode and (b) bare Li electrode. The cells were run at a current density of 2 mA cm^{-2} and a capacity of 2 mAh cm^{-2}. (c) Tafel curves of LiZn-Li and bare Li symmetric cells. EIS spectra of symmetric cells with (d) LiZn-Li electrode and (e) bare Li electrode at different standing time.

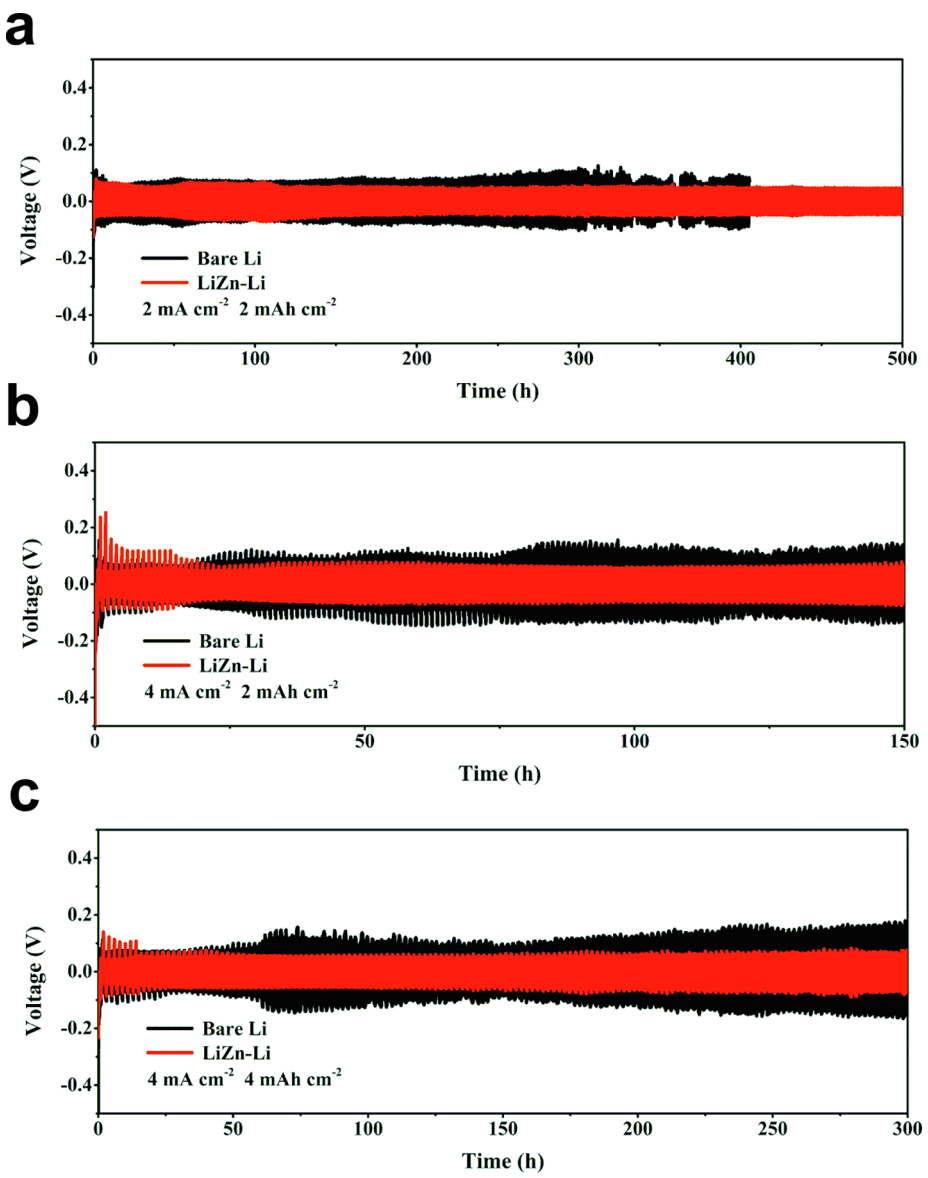

Fig. 3. Comparison of Li plating/stripping performance of bare Li (black) and LiZn-Li (red) symmetric cells. (a) Current density of 2 mA cm^{-2} and capacity of 2 mAh cm^{-2}. (b) Current density of 4 mA cm^{-2} and capacity of 2 mAh cm^{-2}. (c) Current density of 4 mA cm^{-2} and capacity of 4 mAh cm^{-2}. (For interpretation of the references to colour in this figure legend, the reader is referred to the web version of this article.)

stably for more than 500 h at a current density of 2 mA cm^{-2}. This work provides a practical route to improving the electrochemical performance of Li metal anodes.

2. Experimental section

2.1. Pretreatment of Li metal foil

A lithium foil was polished until its surface was extremely shiny and then immersed in a solution of 0.1 M ZnTFS (Acmec) and tetrahydrofuran (THF, Aladdin) for 20 s. The Li foil was washed with THF solvent and dried at room temperature for 24 h under vacuum. All of these operations were conducted in an argon-filled glove box with H_2O and O_2 concentrations of less than 0.5 ppm.

2.2. Material characterization

X-ray diffraction (XRD) measurements were made using a Rigaku X-ray diffractometer with Cu Kα radiation. The surface morphology and structure of the Li foil were observed by scanning electronic microscopy (SEM, Hitachi S-4800).

2.3. Electrochemical measurements

CR2032 coin cells were assembled for electrochemical tests in an argon-filled glove box with less than 0.5 ppm of H_2O and O_2. Symmetric cells (with bare Li foil on each side or ZnTFS-treated Li foil on each side) were assembled to study the Li plating/stripping and perform electrochemical impedance spectroscopy (EIS). The electrolyte was 1 M lithium bis(trifluoromethane)sulfonimide in dioxolane and dimethoxyethane (v/v = 1:1), and 80 μL of electrolyte was added to each cell; the separators were Celgard 2400. Li plating/stripping tests were conducted at 25 °C using a NEWARE multichannel battery tester. EIS measurements were performed on a Solartron frequency analyzer in a frequency range of 0.1 Hz to 100 kHz using a two-electrode system. The Tafel curves and exchange current density of the bare Li and modified Li symmetric cells were measured using a CHI660E electrochemical workstation at a scan rate of 1 mV s^{-1} from −0.13 to 0.13 V.

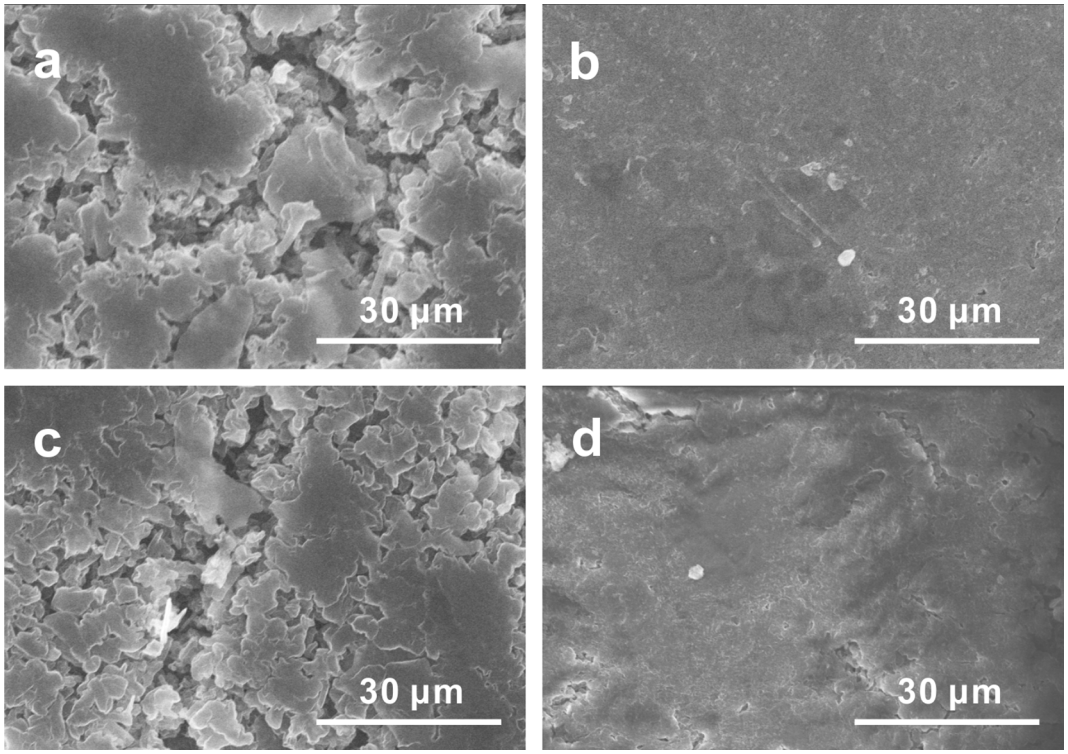

Fig. 4. SEM images of surface morphology of bare Li and LiZn-Li in symmetric cells after different numbers of cycles. (a) Bare Li electrode and (b) LiZn-Li electrode after 20 cycles. (c) Bare Li electrode and (d) LiZn-Li electrode after 40 cycles. The cells were run at a current density of 2 mA cm^{-2} and a capacity of 2 mAh cm^{-2}.

3. Results and discussion

Fig. 1a shows the XRD patterns of bare Li foil and ZnTFS-treated Li foil (LiZn-Li). The diffraction peaks of the Li–Zn alloy phase are detected on the LiZn-Li foil, and peaks at 24.7°, 40.9°, and 48.4° correspond well to the (1 1 1), (2 2 0), and (3 1 1) faces of the Li–Zn alloy, respectively, confirming that Li–Zn alloy formed via the reaction of ZnTFS with bare Li metal. Fig. 1b displays SEM images of the surface morphology of the LiZn-Li foil. The chemical composition is analyzed by energy-dispersive spectroscopy (EDS), as shown in Fig. 1c. Zn is homogeneously distributed on the surface of the LiZn-Li foil. Fig. 1d shows that the thickness of the Li–Zn alloy layer is approximately 12.5 μm. Thus, it can be concluded that a uniform Li–Zn alloy layer was successfully introduced on the surface of the Li foil by simple treatment with ZnTFS. In addition, the XRD pattern of the cycled LiZn-Li electrode indicates that the alloy phase remains after cycling (Fig. 1e).

The EIS spectra of the symmetric cells were obtained to observe the evolution of the interfacial impedance of the LiZn-Li and bare Li electrodes in different cycles. As shown in Fig. 2a and b, the interfacial impedance (R_i) of the bare Li electrode is much larger than that of the LiZn-Li electrode in the first cycle and decreases obviously after 20 cycles. The reason could be that uneven deposition of Li enlarges the contact area between Li metal and the electrolyte [15]. However, the R_i value of the bare Li electrode increases significantly after 40 cycles, indicating degradation of the interface, which is attributed to gradual growth of a resistive surface layer owing to continuous reaction between Li metal and the electrolyte [7,16]. By contrast, the R_i value of the LiZn-Li electrode is smaller than that of the bare Li electrode at every tested cycle. Furthermore, there is almost no noticeable change upon cycling. The smaller resistance of the LiZn-Li electrode can be explained as follows. On one hand, the Li–Zn alloy layer exhibits more rapid charge transfer than the SEI formed on bare Li metal; on the other hand, the reactivity of the Li–Zn alloy with the electrolyte is lower than that of Li metal, which can reduce side reactions between Li metal and the electrolyte, contributing to a stable interface on the Li metal electrode. To further verify the charge transfer kinetics at the interface of the LiZn-Li metal electrode and bare Li electrode, the Tafel curves and exchange current density of the bare Li and LiZn-Li symmetric cells were measured (Fig. 2c). The exchange current density of the LiZn-Li electrode is much higher than that of the bare Li electrode, which suggests better charge transfer capability at the interface [17]. It is known that fast charge transfer at the Li electrode/electrolyte interface can improve the electrochemical reaction kinetics and eliminate uneven Li deposition [17,18]. The higher exchange current density of the LiZn-Li electrode reinforces the finding from the interfacial impedance that the Li–Zn alloy layer on the Li metal electrode facilitates fast charge transfer at the interface. Fig. 2d and e shows the EIS spectra of symmetric cells with LiZn-Li electrode and bare Li electrode at different standing time. After 72 h, the impedance of the bare Li electrode is significantly increased from 108 to 189 Ω, whereas the impedance of the LiZn-Li electrode reveals a slight increase of impedance augment from 48 to 67 Ω. This result confirms that the chemical stability of Li–Zn alloy to the electrolyte is higher than Li metal.

To measure the electrochemical performance of the LiZn-Li electrode, symmetric cells were assembled for galvanostatic cycling tests (Fig. 3). As shown in Fig. 3a, at a current density of 2 mA cm^{-2} and a capacity of 2 mAh cm^{-2}, the hysteresis voltage of the cell with the bare Li electrode gradually increases after 200 h (100 cycles). The increase could be attributed to the unstable SEI, along with continuous consumption of the electrolyte. Repeated breakage and repair of the SEI during charge–discharge cycling increases the SEI thickness and decreases ion transport [4,19]. By contrast, the cell with the LiZn-Li electrode can be cycled stably for over 500 h (250 cycles) with a low hysteresis voltage, indicating that the Li–Zn alloy layer on Li metal can effectively improve the long-cycle stability of the Li metal electrode by providing a stable interface. As the current density increases, the difference in cycle stability becomes more obvious. As the current density is increased to 4 mA cm^{-2}, the hysteresis voltage of the cell with the

bare Li electrode increases and becomes unstable, whereas the cell with the LiZn-Li electrode exhibits a more stable hysteresis voltage (Fig. 3b). The stable hysteresis voltage of the LiZn-Li electrode results from fast charge transfer at the interface and the electrochemical reaction kinetics. Even when the current density is increased to 4 mA cm^{-2} and the plating/stripping capacity is increased to 4 mAh cm^{-2}, the cell with the LiZn-Li electrode still cycles for more than 300 h (150 cycles) with a stable hysteresis voltage, whereas the cell with the bare Li electrode exhibits an unstable hysteresis voltage with a sharp increase (Fig. 3c). This result demonstrates that the Li–Zn alloy layer can also ensure excellent electrochemical cycling performance of the Li metal electrode at a higher current density and capacity. To the best of our knowledge, Li metal electrodes with both higher capacity and higher current density are rarely reported, and stable cycling for over 500 h is one of the best performances among the results of previous studies [20–22].

Finally, SEM was used to observe the surface morphology of the bare Li and LiZn-Li electrodes after repeated Li plating/stripping for 20 and 40 cycles. The surface of the bare Li electrode becomes rough and porous with remarkable formation of dendritic Li after 20 cycles (Fig. 4a), whereas the surface of the LiZn-Li electrode shows deposition of Li with a relatively smooth, dense morphology without dendritic structure (Fig. 4b). After 40 cycles, the surface of the bare Li electrode is rougher, and the Li dendrite growth is more extensive (Fig. 4c). By contrast, the surface of the LiZn-Li electrode remains smooth except for a few cracks (Fig. 4d). This result further suggests that the Li–Zn alloy layer constructed in situ on Li metal improves the electrochemical reaction kinetics at the interface and thus ensures stable uniform deposition of Li. Therefore, the Li–Zn alloy layer plays an extremely significant role in suppressing formation of Li dendrites and improving the long-term electrochemical cycling performance.

4. Conclusion

In summary, a Li–Zn alloy layer is fabricated in situ on Li metal anodes by a simple chemical method. The Li–Zn alloy layer can facilitate fast charge transfer and reaction kinetics at the interface, realizing Li deposition with a smooth, dense morphology and no dendrite formation. Moreover, because the Li–Zn alloy has high chemical resistance to the electrolyte, side reactions between Li metal and the electrolyte can be reduced, contributing to a stable interface on the Li metal anode. As a result, in symmetrical cells, the Li metal anode modified by the Li–Zn alloy layer shows significantly improved long-term electrochemical cycling performance and can cycle stably for more than 500 h. This work demonstrates a simple and useful method to suppress Li dendrite formation by in-situ construction of a Li–Zn alloy layer on Li metal anodes.

Acknowledgments

The authors gratefully acknowledge financial support from the National Natural Science Foundation of China (Grant No. 21875195 and No. 21621091), the Fundamental Research Funds for the Central Universities (20720190040), and the National Key Research and Development Program of China (2017YFB0102000). The authors also express their thanks to Prof. D. W. Liao for his valuable suggestions.

References

[1] J.B. Goodenough, Y. Kim, Challenges for rechargeable Li batteries, Chem. Mater. 22 (2010) 587–603.
[2] S. Chu, Y. Cui, N. Liu, The path towards sustainable energy, Nat. Mater. 16 (2016) 16–22.
[3] A. Basile, A.F. Hollenkamp, A.I. Bhatt, A.P. O'Mullane, Extensive charge-discharge cycling of lithium metal electrodes achieved using ionic liquid electrolytes, Electrochem. Commun. 27 (2013) 69–72.
[4] D. Lin, Y. Liu, Y. Cui, Reviving the lithium metal anode for high-energy batteries, Nat. Nanotechnol. 12 (2017) 194–206.
[5] X.B. Cheng, R. Zhang, C.Z. Zhao, Q. Zhang, Toward safe lithium metal anode in rechargeable batteries: a review, Chem. Rev. 117 (2017) 10403–10473.
[6] K. Liu, A. Pei, H.R. Lee, B. Kong, N. Liu, D. Lin, Y. Liu, C. Liu, P.C. Hsu, Z. Bao, Lithium metal anodes with an adaptive "solid-liquid" interfacial protective layer, J. Am. Chem. Soc. 139 (2017) 4815–4820.
[7] Y. Guo, H. Li, T. Zhai, Reviving lithium-metal anodes for next-generation high-energy batteries, Adv. Mater. 29 (2017) 1700007.
[8] T. Liu, J. Hu, C. Li, Y. Wang, Unusual conformal Li plating on alloyable nanofiber frameworks to enable dendrite suppression of Li metal anode, ACS Appl. Energy Mater. 2 (2019) 4379–4388.
[9] J. Guo, Z. Wen, M. Wu, J. Jin, Y. Liu, Vinylene carbonate-$LiNO_3$: a hybrid additive in carbonic ester electrolytes for SEI modification on Li metal anode, Electrochem. Commun. 51 (2015) 59–63.
[10] Y. Yang, J. Xiong, S. Lai, R. Zhou, M. Zhao, H. Geng, Y. Zhang, Y. Fang, C. Li, J. Zhao, Vinyl ethylene carbonate as an effective SEI-forming additive in carbonate-based electrolyte for lithium-metal anodes, ACS Appl. Mater. Interfaces 11 (2019) 6118–6125.
[11] Q. Yang, C. Li, Li metal batteries and solid state batteries benefiting from halogen-based strategies, Energy Storage Mater. 14 (2018) 100–117.
[12] S. Qu, W. Jia, Y. Wang, C. Li, Z. Yao, K. Li, Y. Liu, W. Zou, F. Zhou, Z. Wang, J. Li, Air-stable lithium metal anode with sputtered aluminum coating layer for improved performance, Electrochim. Acta 317 (2019) 120–127.
[13] W. Tang, X. Yin, S. Kang, Z. Chen, B. Tian, S.L. Teo, X. Wang, X. Chi, K.P. Loh, H.W. Lee, G.W. Zheng, Lithium silicide surface enrichment: a solution to lithium metal battery, Adv. Mater. (2018) e1801745.
[14] R.S. Thompson, D.J. Schroeder, C.M. López, S. Neuhold, J.T. Vaughey, Stabilization of lithium metal anodes using silane-based coatings, Electrochem. Commun. 13 (2011) 1369–1372.
[15] D. Lu, Y. Shao, T. Lozano, W.D. Bennett, G.L. Graff, B. Polzin, J. Zhang, M.H. Engelhard, N.T. Saenz, W.A. Henderson, P. Bhattacharya, J. Liu, J. Xiao, Failure mechanism for fast-charged lithium metal batteries with liquid electrolytes, Adv. Energy Mater. 5 (2015) 1400993.
[16] R. Younesi, M. Hahlin, M. Roberts, K. Edström, The SEI layer formed on lithium metal in the presence of oxygen: a seldom considered component in the development of the Li-O_2 battery, J. Power Sources 225 (2013) 40–45.
[17] J. Meng, F. Chu, J. Hu, C. Li, Liquid polydimethylsiloxane grafting to enable dendrite-free Li plating for highly reversible Li-metal batteries, Adv. Funct. Mater. 29 (2019) 1902220.
[18] Z. Tu, S. Choudhury, M.J. Zachman, S. Wei, K. Zhang, L.F. Kourkoutis, L.A. Archer, Fast ion transport at solid-solid interfaces in hybrid battery anodes, Nat. Energy 3 (2018) 310–316.
[19] L. Wang, Z. Zhou, X. Yan, F. Hou, L. Wen, W. Luo, J. Liang, S.X. Dou, Engineering of lithium-metal anodes towards a safe and stable battery, Energy Storage Mater. 14 (2018) 22–48.
[20] H. Kim, J.T. Lee, D.-C. Lee, M. Oschatz, W.I. Cho, S. Kaskel, G. Yushin, Enhancing performance of Li-S cells using a Li–Al alloy anode coating, Electrochem. Commun. 36 (2013) 38–41.
[21] F. Chu, J. Hu, J. Tian, X. Zhou, Z. Li, C. Li, In situ plating of porous Mg network layer to reinforce anode dendrite suppression in Li-metal batteries, ACS Appl. Mater. Interfaces 10 (2018) 12678–12689.
[22] A.C. Kozen, C.-F. Lin, O. Zhao, S.B. Lee, G.W. Rubloff, M. Noked, Stabilization of lithium metal anodes by hybrid artificial solid electrolyte interphase, Chem. Mater. 29 (2017) 6298–6307.